Supplementary Information

Multiple glutathione disulfide removal pathways mediate cytosolic redox homeostasis

Bruce Morgan[1], Daria Ezeriņa[1], Theresa N.E. Amoako[1], Jan Riemer[2], Matthias Seedorf[3] and Tobias P. Dick[1]*

[1]Division of Redox Regulation, DKFZ-ZMBH Alliance, German Cancer Research Center (DKFZ), Im Neuenheimer Feld 280, 69120 Heidelberg, Germany

[2]Cellular Biochemistry, University of Kaiserslautern, Erwin-Schrödinger-Str. 13, 67663 Kaiserslautern, Germany

[3]Zentrum für Molekulare Biologie der Universität Heidelberg (ZMBH), DKFZ-ZMBH Alliance, Im Neuenheimer Feld 282, 69120 Heidelberg, Germany

*Corresponding Author

Tel.: +49-6221-42-2320

Fax: +49-6221-42-4406

Email: t.dick@dkfz.de

Nature Chemical Biology: doi:10.1038/nchembio.1142

Supplementary Results

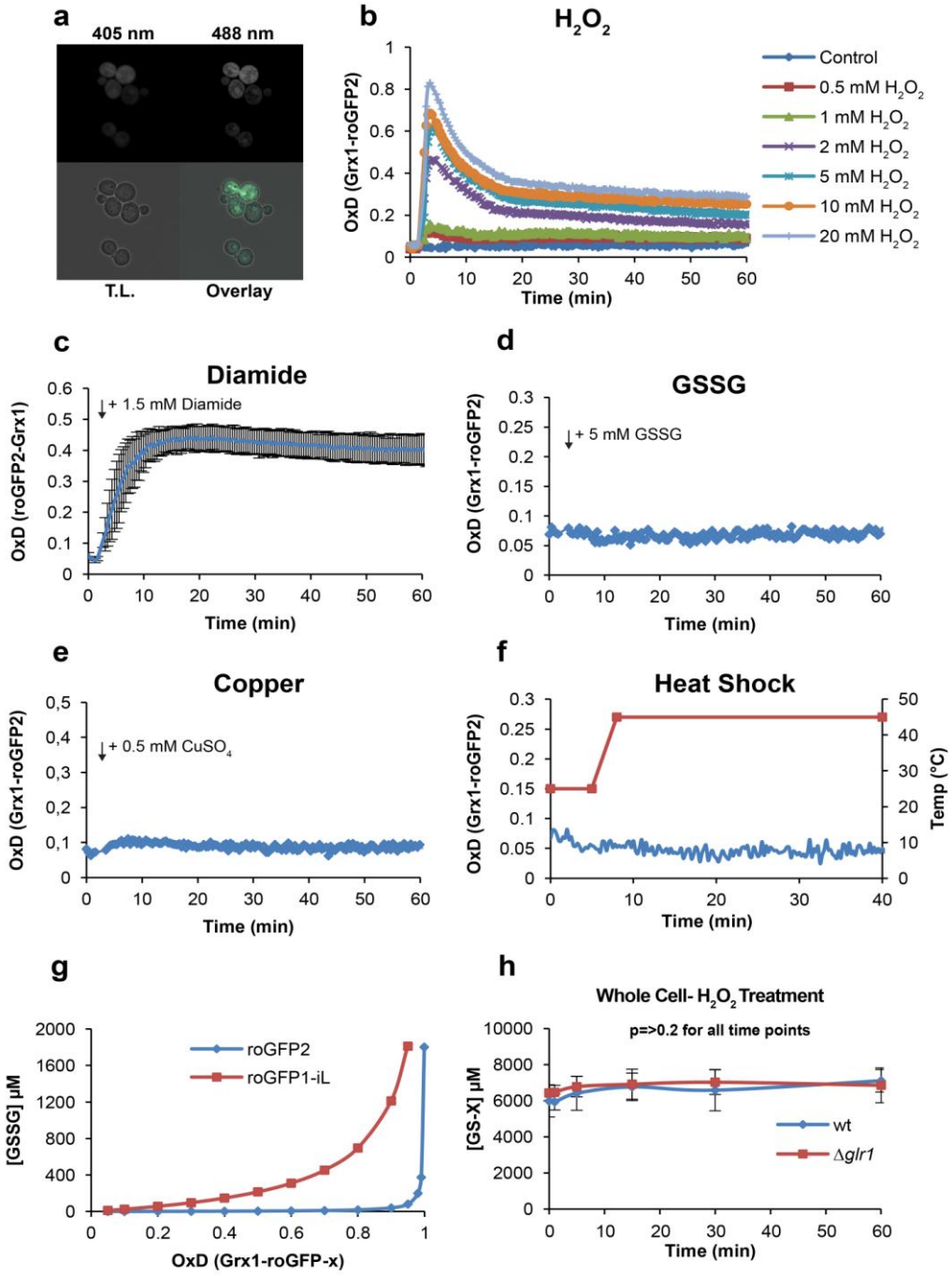

Supplementary Figure 1. Related to main Figures 1 and 2. The cytosolic glutathione pool is robustly resistant to perturbation.

(a) Fluorescence microscopy image, showing roGFP2-Grx1 probe emission at 405 nm and 488 nm in a wt cell, as well as transmitted light (T.L.) and an image overlay. (b–f) Cytosolic E_{GSH} response as measured with the Grx1-roGFP2 probe to the addition of (b) 0.5–20 mM H_2O_2, (c) 1.5 mM diamide, (d) 5 mM GSSG, (e) 0.5 mM copper sulphate, and (f) heat shock. (g) Relationship between the degree

of oxidation (OxD) of the roGFP2 and roGFP1-iL probes and the GSSG concentration assuming a 10 mM total glutathione pool. (h) Related to main Fig. 2e. Time course of the change in whole cell GS-X concentration measured in lysates prepared from wt and Δ*glr1* cells. Samples were removed and immediately processed at the indicated time points following the addition of 1 mM H_2O_2 (n=3).

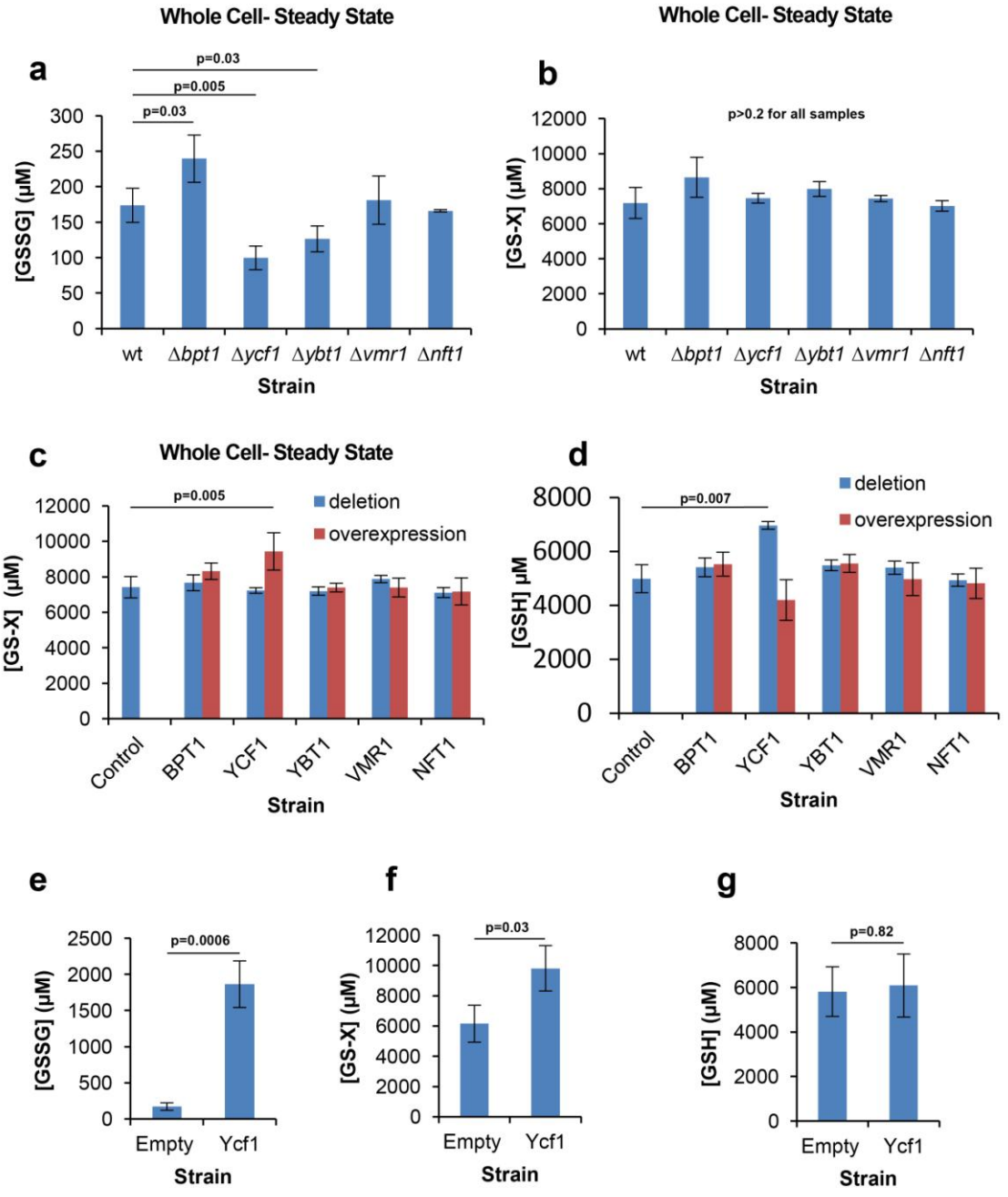

Supplementary Figure 2. Related to main Figures 3 and 4. Ycf1 mediates vacuolar accumulation of cytosolic GSSG.

(a–b) Whole cell GSSG (a) and total glutathione (GS-X) (b) levels in cells deleted for each of the vacuolar ABC-C transporters (n=3–5). (c–d) Complementary to **Fig. 3a.** Whole cell steady state GS-X (c) and GSH levels (d) in Δ*glr1* strains further deleted for or overexpressing each of the vacuolar ABC-C transporters (n=3–5). (e–g) Whole cell GSSG (e), total glutathione (GS-X) (f), and GSH (g) levels in Δ*glr1*Δ*ycf1* cells expressing either an empty p416TEF vector (Empty) or p416TEF-*YCF1* (Ycf1) (n=6).

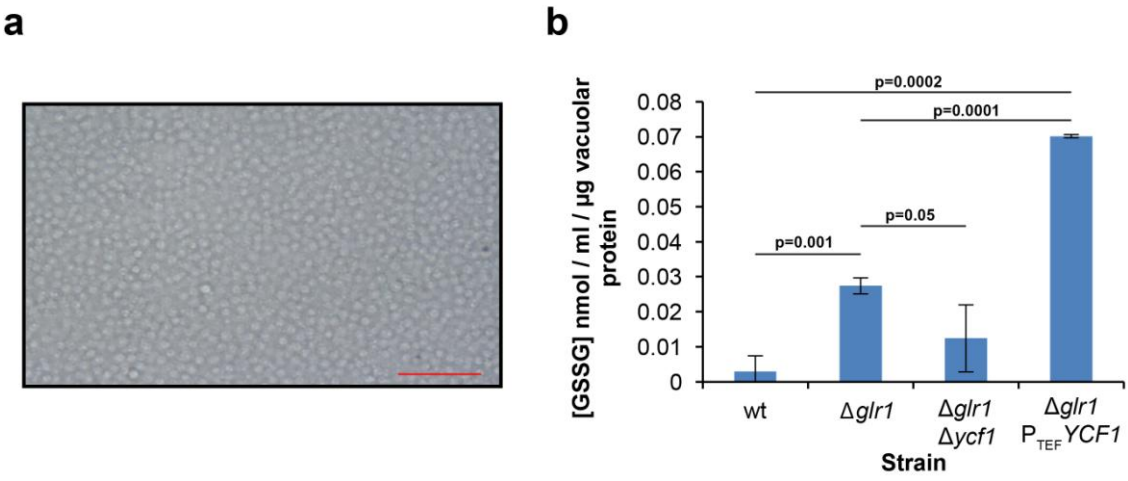

Supplementary Figure 3. GSSG measurement in a highly enriched vacuolar fraction

(a) Microscopy image of enriched vacuolar fraction. Scale bar = 10 µm, for comparison see also the microscopy image of ultra-pure yeast vacuoles in Wiederhold et al, 2009 [1] (n=3). (b) GSSG concentration measured in enriched vacuolar fractions, isolated from wt, Δ*glr1*, Δ*glr1*Δ*ycf1* and Δ*glr1*P_{TEF}*YCF1* strains.

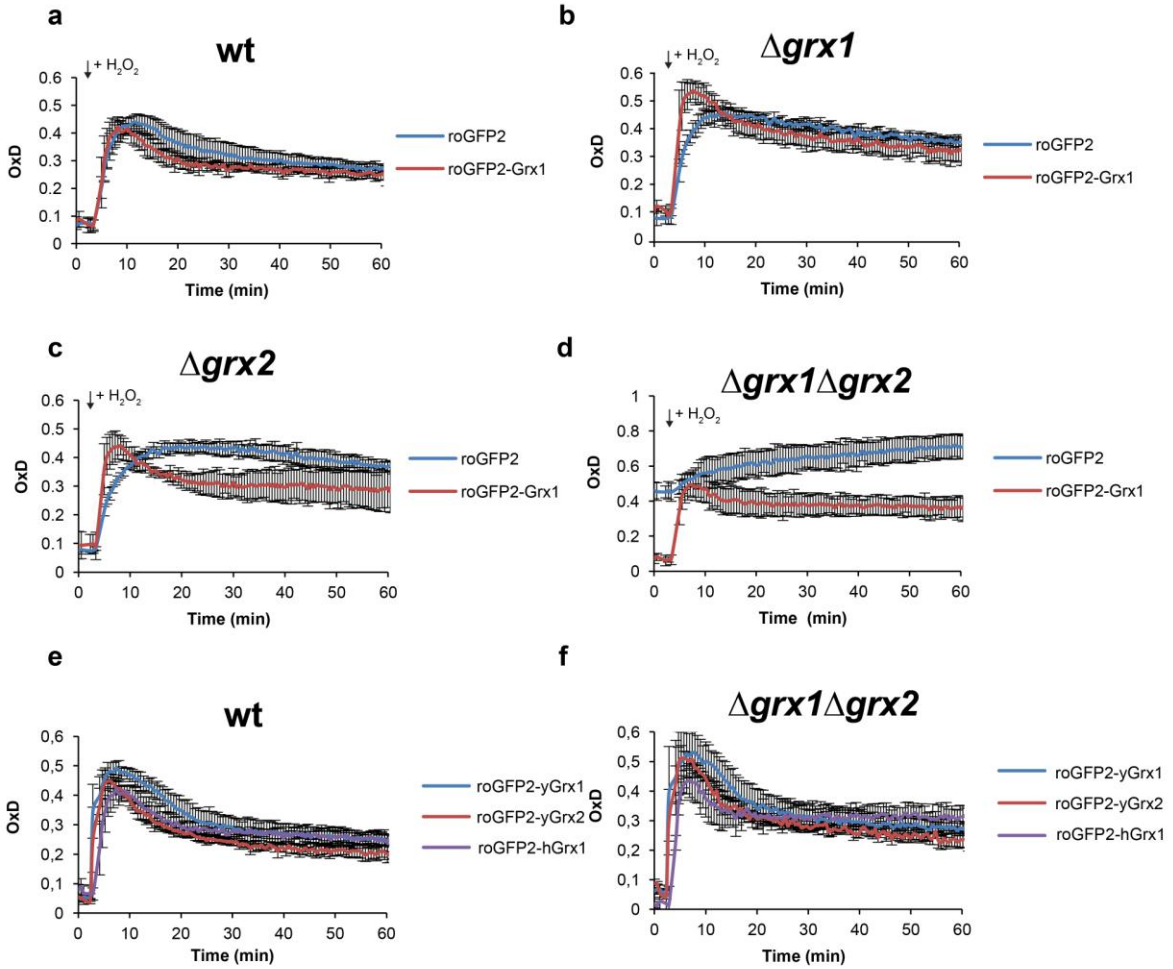

Supplementary Figure 4. roGFP2 equilibration is strictly dependent upon the presence of a dithiol glutaredoxin.

(a–d) roGFP2 strictly requires a dithiol Grx to equilibrate with the glutathione redox couple. Response of roGFP2 and roGFP2-Grx1 probes to the addition of 5 mM H_2O_2 in (a) wt, (b) Δ*grx1*, (c) Δ*grx2*, or (d) Δ*grx1*Δ*grx2* cells (n=3). (e–f) roGFP2-yeastGrx fusion probes equilibrate with the cytosolic glutathione redox couple with equal efficiency to the roGFP2-humanGrx1 probe. Response of roGFP2-Grx1, roGFP2-yeastGrx1 and roGFP2-yeastGrx2 probes to the addition of 5 mM H_2O_2 in (e) wt and (f) Δ*grx1*Δ*grx2* cells (n=3).

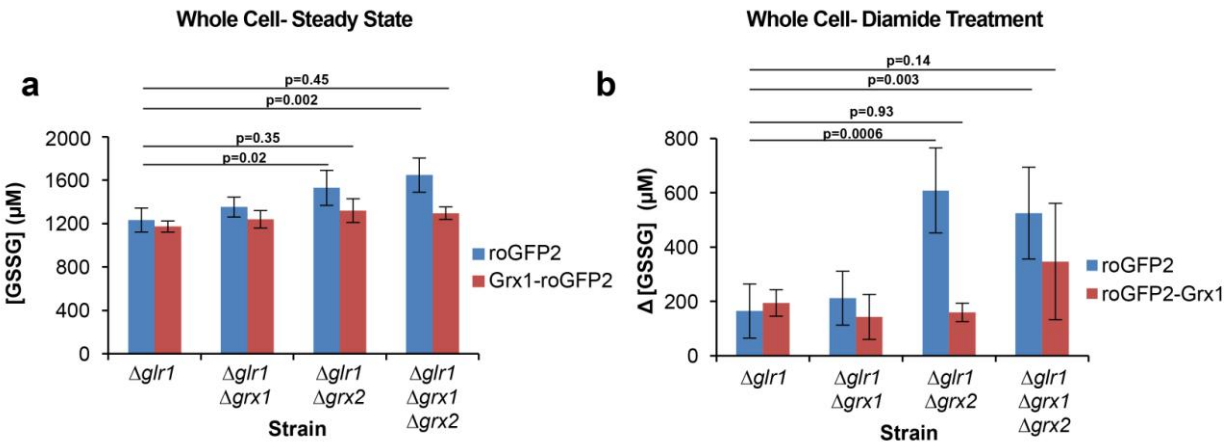

Supplementary Figure 5. roGFP2-Grx1 expression does not significantly impact upon whole cell GSSG levels, but can compensate for the absence of endogenous Grxs.

(a) GSSG levels at steady state in Δ*glr1*, Δ*glr1*Δ*grx1*, Δ*glr1*Δ*grx2* and Δ*glr1*Δ*grx1*Δ*grx2* cells transformed with either a roGFP2 or roGFP2-Grx1 probe (n=3). (b) Change in whole cell GSSG levels in the strains in (a) following 60 min treatment with 0.33 mM diamide (n=3).

Nature Chemical Biology: doi:10.1038/nchembio.1142

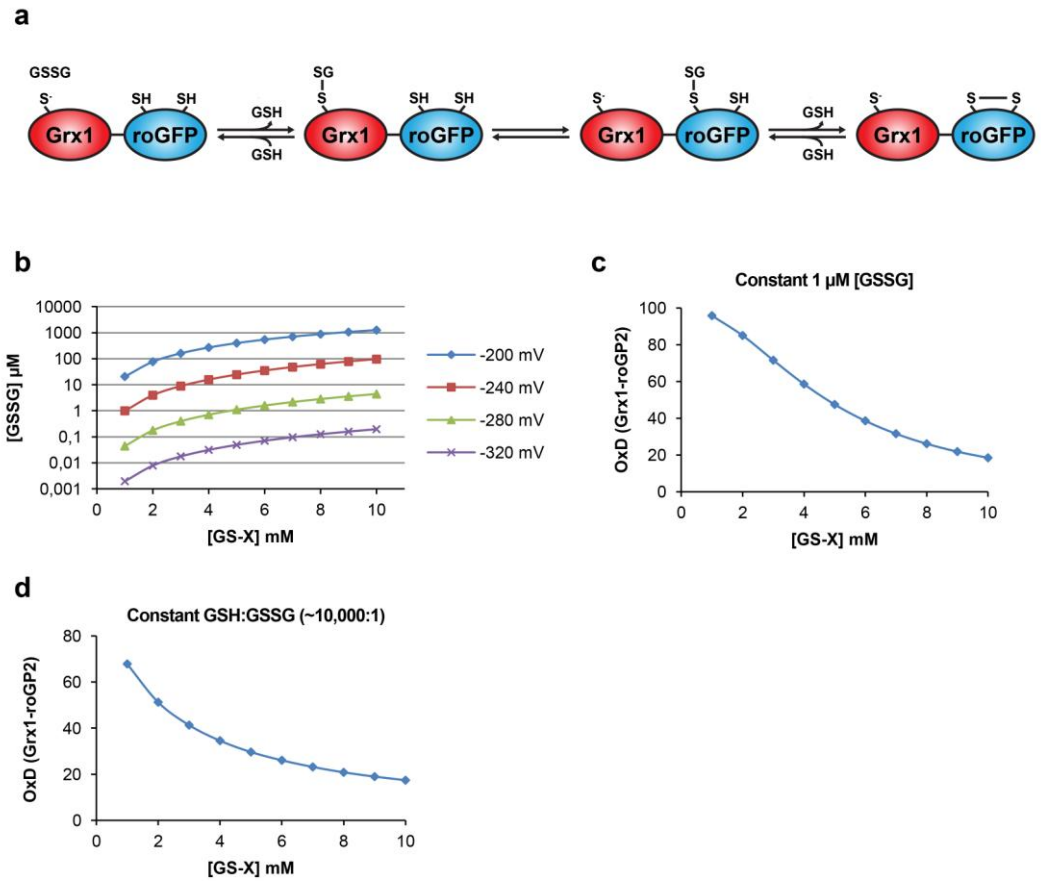

Supplementary Figure 6. Considerations for the interpretation of roGFP-based probe data.

(a) Cartoon illustrating the mechanism of the Grx1-roGFP2 probe. (b) Graph illustrating the relationship between [GS-X] and [GSSG] at various constant E_{GSH} values. (c) Graph illustrating the effect of changing [GS-X] on OxD_{roGFP2}, when [GSSG] is constant. (d) Plot of the effect of changing [GS-X] on OxD_{roGFP2} when GSH:GSSG is constant.

Nature Chemical Biology: doi:10.1038/nchembio.1142

Supplementary Table 1. Yeast strains used in this study.

Strain	Genotype	Source
BY4741	*MAT*a *his3Δ1 leu2Δ0 met15Δ0 ura3Δ0*	Euroscarf
BY4742	*MAT*α *his3Δ1 leu2Δ1 lys2Δ0 ura3Δ0*	Euroscarf
YPH499	*MAT*a *ura3-52 lys2-801_amber ade2-101_ochre trp1-Δ63 his3-Δ200 leu2-Δ1*	Euroscarf
BM1	BY4741 Δ*ycf1*::*kanMX4*	Euroscarf
BM2	BY4742 Δ*glr1*::*kanMX4*	Euroscarf
BM3	BY4742 Δ*bpt1*::*kanMX4*	Euroscarf
BM4	BY4742 Δ*ycf1*::*kanMX4*	Euroscarf
BM5	BY4742 Δ*ybt1*::*kanMX4*	Euroscarf
BM6	BY4742 Δ*vmr1*::*kanMX4*	Euroscarf
BM7	BY4742 Δ*nft1*::*kanMX4*	Euroscarf
BM8	BY4742 Δ*glr1*::*kanMX4* Δ*bpt1*::*natNT2*	This Study
BM9	BY4742 Δ*glr1*::*kanMX4* Δ*ycf1*::*kanMX4*	This Study
BM10	BY4742 Δ*glr1*::*kanMX4* Δ*ybt1*::*natNT2*	This Study
BM11	BY4742 Δ*glr1*::*kanMX4* Δ*vmr1*::*natNT2*	This Study
BM12	BY4742 Δ*glr1*::*kanMX4* Δ*nft1*::*natNT2*	This Study
BM13	BY4742 Δ*glr1*::*kanMX4* P_{TEF}-*BPT1*::*natNT2*	This Study
BM14	BY4742 Δ*glr1*::*kanMX4* P_{TEF}-*YCF1*::*natNT2*	This Study
BM15	BY4742 Δ*glr1*::*kanMX4* P_{TEF}-*YBT1*::*natNT2*	This Study
BM16	BY4742 Δ*glr1*::*kanMX4* P_{TEF}-*VMR1*::*natNT2*	This Study
BM17	BY4742 Δ*glr1*::*kanMX4* P_{TEF}-*NFT1*::*natNT2*	This Study
BM18	BY4742 Δ*glr1*::*kanMX4* Δ*trx1*::*hphNT1*	This Study
BM19	BY4742 Δ*glr1*::*kanMX4* Δ*trx2*::*hphNT1*	This Study
BM20	BY4742 Δ*glr1*::*kanMX4* Δ*ycf1*::*kanMX4* Δ*trx1*::*hphNT1*	This Study
BM21	BY4742 Δ*glr1*::*kanMX4* Δ*ycf1*::*kanMX4* Δ*trx2*::*hphNT1*	This Study
BM22	BY4742 Δ*glr1*::*kanMX4* Δ*ycf1*::*kanMX4* Δ*grx2*::*natNT2*	This Study
BM23	BY4742 Δ*glr1*::*kanMX4* Δ*ycf1*::*kanMX4* Δ*trx1*::*hphNT1* Δ*grx2*::*natNT2*	This Study
BM24	BY4742 Δ*glr1*::*kanMX4* Δ*ycf1*::*kanMX4* Δ*trx2*::*hphNT1* Δ*grx2*::*natNT2*	This Study
BM25	YPH499 Δ*grx1*::*URA3*	This Study
BM26	YPH499 Δ*grx2*::*kanMX4*	This Study
BM27	YPH499 Δ*grx1*::*URA3* Δ*grx2*::*kanMX4*	This Study
BM28	YPH499 Δ*glr1*::*natNT2*	This Study
BM29	YPH499 Δ*glr1*::*natNT2* Δ*grx1*::*URA3*	This Study
BM30	YPH499 Δ*glr1*::*natNT2* Δ*grx2*::*kanMX4*	This Study
BM31	YPH499 Δ*glr1*::*natNT2* Δ*grx1*::*URA3* Δ*grx2*::*kanMX4*	This Study

Supplementary Table 2. Plasmids used in this study.

Plasmid	Description	Source
pBM1	p415 TEF Empty	(2)
pBM2	p416 TEF Empty	(2)
pBM5	p415 TEF Grx1-roGFP2	This Study
pBM3	p415 TEF roGFP2(yeast codon optimized)	This Study
pBM4	p415 TEF roGFP2(yeast codon optimized)-Grx1	This Study
pBM5	p415 TEF roGFP1-iL-Grx1	This Study
pBM6	p416 TEF *YCF1*	This Study
pBM7	p415 TEF roGFP2(yeast codon optimized)-yeastGrx1	This Study
pBM8	p415 TEF roGFP2(yeast codon optimized)-yeastGrx2	This Study

Nature Chemical Biology: doi:10.1038/nchembio.1142

Supplementary References

1. Wiederhold, E. et al. The yeast vacuolar membrane proteome. *Mol Cell Proteomics* **8**, 380-92 (2009).

2. Mumberg, D., Muller, R. & Funk, M. Yeast vectors for the controlled expression of heterologous proteins in different genetic backgrounds. *Gene* **156**, 119-22 (1995).